Atmospheric O_2/N_2 changes, 1993–2002: Implications for the partitioning of fossil fuel CO_2 sequestration

Michael L. Bender,[1] David T. Ho,[1] Melissa B. Hendricks,[1] Robert Mika,[1] Mark O. Battle,[2] Pieter P. Tans,[3] Thomas J. Conway,[3] Blake Sturtevant,[1] and Nicolas Cassar[1]

[1] Improvements made to an established mass spectrometric method for measuring changes in atmospheric O_2/N_2 are described. With the improvements in sample handling and analysis, sample throughput and analytical precision have both increased. Aliquots from duplicate flasks are repeatedly measured over a period of 2 weeks, with an overall standard error in each flask of 3–4 per meg, corresponding to 0.6–0.8 ppm O_2 in air. Records of changes in O_2/N_2 from six global sampling stations (Barrow, American Samoa, Cape Grim, Amsterdam Island, Macquarie Island, and Syowa Station) are presented. Combined with measurements of CO_2 from the same sample flasks, land and ocean carbon uptake were calculated from the three sampling stations with the longest records (Barrow, Samoa, and Cape Grim). From 1994–2002, We find the average CO_2 uptake by the ocean and the land biosphere was 1.7 ± 0.5 and 1.0 ± 0.6 GtC yr^{-1} respectively; these numbers include a correction of 0.3 Gt C yr^{-1} due to secular outgassing of ocean O_2. Interannual variability calculated from these data shows a strong land carbon source associated with the 1997–1998 El Niño event, supporting many previous studies indicating that high atmospheric growth rates observed during most El Niño events reflect diminished land uptake. Calculations of interannual variability in land and ocean uptake are probably confounded by non-zero annual air sea fluxes of O_2. The origin of these fluxes is not yet understood.

Citation: Bender, M. L., D. T. Ho, M. B. Hendricks, R. Mika, M. O. Battle, P. P. Tans, T. J. Conway, B. Sturtevant, and N. Cassar (2005), Atmospheric O_2/N_2 changes, 1993–2002: Implications for the partitioning of fossil fuel CO_2 sequestration, *Global Biogeochem. Cycles*, *19*, GB4017, doi:10.1029/2004GB002410.

1. Introduction

[2] Studies of the distribution of O_2 in air are playing an increasingly important role in our understanding of the global carbon cycle [e.g., *Intergovernmental Panel on Climate Change*, 2001]. *Keeling and Shertz* [1992] first made systematic, high-precision measurements of the O_2/N_2 ratio of air, with sampling beginning in 1990. Our group began making similar measurements in 1991 [*Bender et al.*, 1994, 1996; *Battle et al.*, 2000]. The two groups currently each measure O_2/N_2 at approximately 14 stations worldwide, intercomparing regularly at three (La Jolla, Cape Grim, and American Samoa). Other groups have undertaken more focused studies of O_2/N_2 [e.g., *Langenfelds et al.*, 1999; *Tohjima et al.*, 2003].

[3] O_2/N_2 measurements are now used to address a variety of issues relevant to carbon geochemistry and ocean circulation. Arguably the most important of these is the partitioning of anthropogenic CO_2 uptake between the land biosphere and the ocean. The O_2/N_2 ratio of air is falling because combustion of fossil fuel and biomass both consume O_2. The observed rate of decrease is less than the calculated rate of O_2 consumption by combustion. The difference is due almost entirely to net O_2 production (and corresponding CO_2 uptake) associated with the growth of the land biosphere. O_2/N_2 data thus allow us to partition the global CO_2 sink between the land biosphere and the ocean. Such calculations were first made by *Keeling and Shertz* [1992], followed by *Keeling et al.* [1996], *Battle et al.* [2000], and others. The most recent summary is from *Manning* [2001], working in the laboratory of R. F. Keeling.

[4] O_2/N_2 ratios of air vary seasonally because of the annual cycle of net production and O_2 uptake by the biosphere. The land biosphere, in the net, produces C_{org} and O_2 in summer and consumes these in winter. O_2 and CO_2 concentrations from this source covary with $\Delta O_2/\Delta CO_2 \sim -1.1$ [*Severinghaus*, 1995]. O_2/N_2 ratios of air also vary seasonally because of ocean carbon fluxes. In the summertime, O_2/N_2 rises because net production in the euphotic

[1]Department of Geoscience, Guyot Hall, Princeton University, Princeton, New Jersey, USA.
[2]Department of Physics and Astronomy, Bowdoin College, Brunswick, Maine, USA.
[3]Climate Monitoring and Diagnostics Laboratory, National Oceanic and Atmospheric Administration, Boulder, Colorado, USA.

Table 1. Locations of Sample Collection Sites

Station Abbreviation	Station Name	Latitude	Longitude	Altitude above sea level, m
BRW	Point Barrow, Alaska, United States	71.32	−156.60	11
SMO	Tutuila, American Samoa	−14.24	−170.57	42
AMS	Amsterdam Island, France	−37.95	77.53	150
CGO	Cape Grim, Tasmania, Australia	−40.68	144.68	94
MAC	Macquarie Island, Australia	−54.50	158.95	12
SYO	Syowa Station, Antarctica, Japan	−69.00	39.58	14

zone supersaturates the mixed layer and induces a transfer to the atmosphere. In the wintertime, O_2/N_2 falls as undersaturated waters mix to the surface and are ventilated. There is no comparable seasonal ocean source of CO_2, largely because of the relative high solubility of CO_2 and the ocean's buffering capacity. The seasonal cycle of O_2 in excess of that of CO_2 (actually $1.1 \times CO_2$) is a reflection of the magnitude of ocean carbon fluxes, and their spatial and interannual variability.

[5] There is also meridional variability in the atmospheric O_2/N_2 ratio (as well as unresolved zonal variability that is not discussed here). This variability reflects the meridional variability in CO_2 input (O_2 consumption) by combustion and net CO_2 uptake (net O_2 production) due to growth of the land biosphere [*Keeling et al.*, 1993]. It also reflects the fundamental pattern of ocean mixing and ventilation [*Stephens et al.*, 1998]. Mixing and ventilation determine where there is C_{org} production, along with net O_2 production and its attendant transfer to the atmosphere. These processes also determine where O_2 deficient waters of the ocean take up O_2 to be resaturated.

[6] Anthropogenic and oceanographic processes introduce O_2 concentration variations that are superimposed on the large background concentration of O_2 in air (nominally 20.95%). The fractional changes in O_2/N_2 are thus small. They must be measured at very high precision to provide useful constraints on anthropogenic carbon fluxes and properties we wish to infer from meridional gradients. The precision required for O_2/N_2 ratio measurements is about ±5 per meg, where 1 per meg = 0.001‰. One can routinely achieve this precision with proper air handling, highly repeatable methods of air collection and analysis, stable standards and an analytical method inherently capable of per meg precision. *Keeling and Shertz* [1992] and *Keeling et al.* [1998] developed appropriate protocols for sample collection and standard storage. Keeling and colleagues developed an interferometer [*Keeling*, 1988], paramagnetic analyzer [*Manning et al.*, 1999], and UV analyzer [*Stephens et al.*, 2003] with the required precision. Recently, a gas chromatographic method has been developed for O_2/N_2 [*Tohjima*, 2000; *Tohjima et al.*, 2003].

[7] *Bender et al.* [1994, 1996] adopted the sampling and standard storage methodologies of *Keeling and Shertz* [1992] and *Keeling et al.* [1998], and showed that O_2/N_2 could also be accurately measured by an off-the-shelf isotope ratio mass spectrometer. *Bender et al.* [1996] and *Battle et al.* [2000] described two sample-handling protocols. One uses the standard dual viscous inlet and compares the O_2/N_2 of a sample and a standard processed in the identical manner [*Bender et al.*, 1994, 1996]. The second uses a custom sample side inlet, to compare sample and standard gases with an arbitrary reference gas [*Battle et al.*, 2000]. This second inlet design was originally implemented in 1994 with a vacuum manifold to which four flasks could be attached and analyzed under computer control. In 1998, it was replaced with the current version, a vacuum manifold connected to a carousel. Twelve sample flasks can be mounted on the carousel and again analyzed sequentially under computer control. In this paper, we describe these sample processing lines, the protocols for interpreting and applying standard data, procedures for calculating sample O_2/N_2 ratios, and the attendant uncertainties.

[8] O_2/N_2 data of our group have been published through the year 1998 [*Battle et al.*, 2000]. Here we extend these results to the end of 2002, and compare estimates of land and ocean CO_2 uptake with results of other recent studies.

[9] As noted above, we can use atmospheric O_2/N_2 data to partition anthropogenic CO_2 sequestration between the land biosphere and the ocean. In its simplest form, this calculation assumes that the annually averaged oceanic O_2 inventory is constant. However, this inventory is likely to be changing, for two reasons. First, the ocean is warming [*Levitus et al.*, 2000], reducing gas solubility and driving O_2 from ocean to atmosphere [*Keeling and Garcia*, 2002]. Second, changes in oceanic stratification may be altering the oceanic carbon cycle. These carbon cycle changes would likely be accompanied by the transfer of O_2 between ocean and atmosphere.

[10] We calculate anthropogenic CO_2 sequestration rates by the ocean and the land biosphere assuming a constant oceanic O_2 inventory. We then summarize estimates of the rate at which the oceanic O_2 inventory is changing, and associated changes in calculated anthropogenic CO_2 sequestration rates. Finally, we examine interannual variability in land and ocean CO_2 sequestration.

2. Methods

[11] Locations of our six sampling sites with the longest records (Point Barrow, American Samoa, Cape Grim, Amsterdam Island, Macquarie Island, and Syowa Station; Table 1) are shown in Figure 1. Barrow is in the Northern Hemisphere, while the other five are in the Southern Hemisphere. O_2/N_2 and CO_2 data from these sites are presented here.

[12] Following *Keeling and Shertz* [1992], the differences in O_2/N_2 are expressed in per meg units,

$$\delta(O_2/N_2) = \left(\frac{(O_2/N_2)_{sample}}{(O_2/N_2)_{standard}} - 1 \right) \times 10^6, \qquad (1)$$
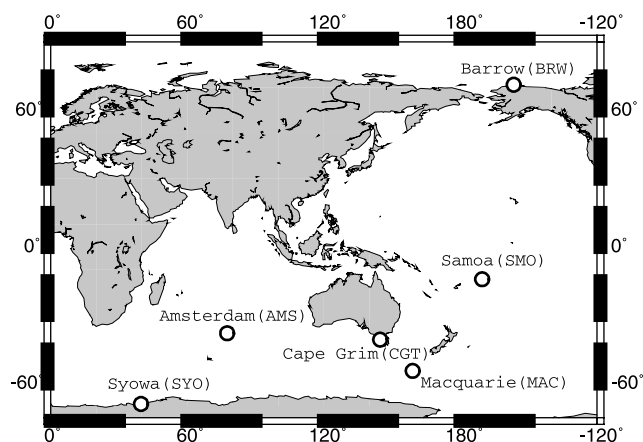
Figure 1. Location of O$_2$/N$_2$ sampling stations.

where (O$_2$/N$_2$)$_{sample}$ is the measured O$_2$/N$_2$, and (O$_2$/N$_2$)$_{standard}$ is an arbitrary standard gas, GF 1 [*Bender et al.*, 1996]. GF 1 was our original standard, contained in a 70-L flask, and is now a virtual standard only. In this formulation, a change of 1 ppm in the atmospheric mole fraction is equivalent to 4.8 per meg.

[13] Samples were collected in 2-L glass flasks sealed by Louwers-Hapert shaft seal O-ring valves [*Bender et al.*, 1996]. The O$_2$/N$_2$ ratio may be altered by preferential diffusion of O$_2$ through the Viton O-rings during storage [*Sturm et al.*, 2004]. The O$_2$/N$_2$ changes are minimized for our samples, which are collected at sea level, indoors, at ambient atmospheric pressure. Diffusion still exerts some influence, however, because there will always be some difference between pressures of O$_2$ and N$_2$ in the flask and in the storage room. Assuming a pressure difference of up to 3%, tests in our lab indicate that a sample stored typically for 100 days to analysis could vary by up to 3 per meg. Samples from Syowa are collected from February to the following January, and returned thereafter. These samples are stored for 4–16 months prior to analysis, and their O$_2$/N$_2$ ratio could be altered by up to 16 per meg according to our calculation. However, there is no discontinuity between January samples (stored for about 4 months) and February samples (stored for about 16 months (Figure 5 in section 3). At this site, a close match between storage and collection conditions apparently eliminates the potential artifact from diffusion.

2.1. Overview of Analytical Methods

[14] O$_2$/N$_2$ was measured by isotope ratio mass spectrometry. The required precision and long-term reproducibility, of order ±5 per meg (±0.005‰), are readily achieved by the instrument, but pose considerable challenges to sample handling. We constructed custom inlet lines leading to the changeover valves of the mass spectrometer. Two inlet lines were used for analyzing samples at the University of Rhode Island (URI) and one at Princeton University. Samples collected in 1999 and later were analyzed at Princeton.

[15] In the "first URI method" [*Bender et al.*, 1996], samples were analyzed by direct comparison with standards. In the "second URI method," and in the "Princeton

method," samples and standards were independently analyzed against a common reference gas. In both cases, the reference gas was dry air in a 70-L cylindrical glass flask filled to a nominal pressure of 1 atmosphere. A fused SiO$_2$ capillary tube (25 μm i.d., ∼1 m long) was inserted through a Vespel® ferrule and glass tube so that one end was positioned in the center of the reference flask. The other end was attached with a Vespel® ferrule into the reference side of the changeover valve of the mass spectrometer.

[16] Sample and standard gases were admitted to a glass vacuum manifold with valves leading to pumps, sample/standard ports, and a ∼30 cm^3 glass cylinder. The gases were expanded into the cylinder at 1 atmosphere nominal pressure. An aluminum piston, riding in the cylinder and sealed with 2 Viton™ O-rings, was moved to adjust the pressure so that the ion current of the sample matched the ion current of the reference to ∼0.1%. An appropriate correction, of order 1–2 per meg, was made for the pressure imbalance. The inlet system was enclosed in a large glass and wood box to stabilize the temperature. All valves were Louwers-Hapert shaft seal valves with Viton™ O-rings.

[17] We employed eight standards against which samples were compared. Each standard was dry air from Niwot Ridge, Colorado, and was stored in a high-pressure aluminum cylinder. Four were designated "working standards" (Table 2), and four were designated "stability standards." One aliquot of stability standard 1069 was also used as a working standard. Air was transferred from each cylinder to a 70-L glass flask, to a nominal pressure of 1.1 atmospheres. Transfers were done at a flow rate of 4–10 L min^{-1} through 5 m × 0.125″ o. d. stainless tubing. These 70-L flasks could be attached to the inlet line and aliquots drawn for analysis. Each "working standard" was analyzed in triplicate once per week, while each "stability standard" was analyzed in triplicate once per month. Standard curves (Figure 2, and see more detailed discussion below) were determined from working standards alone. Results for stability standards were used to ascertain the rate of drift in the standard curves. The curves of O$_2$/N$_2$ versus time from the stability standards were collapsed onto a single standard curve, by subtracting the difference between the O$_2$/N$_2$ ratio of each standard and GF1 [*Bender et al.*, 1996]. The short-term variability in the standard curve is then due to random errors in the individual analyses. Long-term variability is due to drift in the zero enrichment (the hypothetical δ value that would be measured if identical gas were admitted to both sample and reference sides of the mass spectrometer), errors in filling the individual 70-L standard flasks, and errors in accounting for the change in O$_2$/N$_2$ of the standard flasks as aliquots are drawn off for analysis. The first term (change in

Table 2. Working Standards and Their O$_2$/N$_2$ Offsets With Respect to the Virtual Standard GF-1

Working Standard	O$_2$/N$_2$ Offset (per meg)
1069	−163
1514	−21
2706	0
1125	−49
1516	2
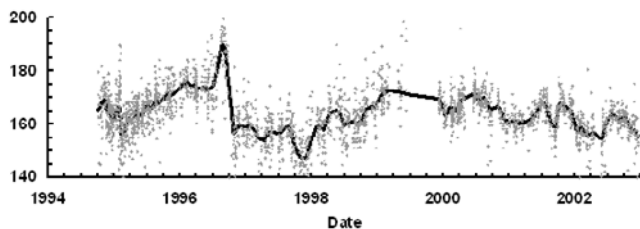
Figure 2. Standard curve, derived solely from the analysis of working standards. Symbols represent individual analyses, while the solid line is the LOESS fit that defines our standard curve.

the zero) is identical for samples and standards, and does not introduce error into the ratios.

[18] There were three important differences between the second URI method and the Princeton method. First, different mass spectrometers were used for the analyses. Second, at URI, four air samples were simultaneously attached to the vacuum manifold; at Princeton, 12 air samples were attached to a "carousel" that connected flasks sequentially to the vacuum line. Third, there were differences in the geometry with which flasks were connected and gas transferred. As a result of these differences, various corrections, described below, differ from one method to the other.

[19] In the following discussion, we describe the measurement protocols, along with the corrections and calculations required to determine O_2/N_2 ratios from the mass spectrometric measurements. The calculation of the standard curve is first described in detail; we then discuss the calculation of sample O_2/N_2 values. Calculation of data involves accounting for differences in O_2/N_2 ratios when samples are admitted from various sample ports, correcting for differences in the O_2/N_2 ratio when samples are admitted from sample vs. standard ports, and correcting for the change in O_2/N_2 ratios measured in sequential analyses. Analytical reproducibility of air in individual flasks needs to be assessed, along with precision of replicate flasks. An essential attribute of both the second URI method and the Princeton method is that all samples and standards are analyzed repeatedly, and with identical procedures.

2.2. Mass Spectrometry

[20] At URI, aliquots of dry air were analyzed with a Finnigan MAT 251 isotope ratio mass spectrometer by simultaneous collection of masses 29 and 32 ($^{14}N^{15}N$ and $^{16}O_2$). Samples were measured for two blocks with 25 cycles (reference/sample/reference changeovers) per block. Standard errors for 1 block were typically ±4 per meg. At Princeton, samples were analyzed for O_2/N_2 (32/28) and Ar/N_2 (40/28) using a Finnigan Delta Plus XL isotope ratio mass spectrometer configured to simultaneously collect any three of the following masses: 28, 29, 32, 33, 34, 36, 38, 40 and 44. We measured 28/32/40 in one block of 16 cycles, which gave O_2/N_2 with standard errors of $1-2$ per meg and Ar/N_2 with standard errors of ~4 per meg. We then measured $\delta^{15}N$ of N_2 and CO_2/N_2 (44/28) in one block of

8 cycles. The O_2/N_2 ratios determined on both instruments were significantly affected by the ion current imbalance between sample and reference sides (corresponding to pressure imbalances in the inlet system). We periodically determined the magnitude of this effect by repeatedly analyzing the same gas with ion currents imbalanced to different amounts. A correction based on the degree of the imbalance was applied to all samples and standards. The magnitude was typically $1-3$ per meg.

2.3. Derivation of the Standard Curve

[21] The 70-L glass flasks, which contain the standards, are fitted with two 9-mm shaft-seal Louwers-Hapert™ valves. Flasks are analyzed $140-280$ times, by which point their pressure has dropped by about 25%. At this point a "new" working standard is created by filling an evacuated 70-L flask with air from the appropriate high-pressure cylinder. "Old" and "new" fills are alternately run for an interim period before the old flask is retired. We observed that O_2/N_2 ratios in aliquots drawn from old fills were systematically lower than values measured from new fills during the same time period. We attribute this difference to fractionation when drawing aliquots of standard gas from 70-L flasks, and make an appropriate "distillation correction" to all standard analyses. The O_2/N_2 ratio added to the measured value for each sequential analysis is +0.0226 per meg/aliquot analyzed at URI, and +0.0097 per meg/aliquot at Princeton.

[22] The 70-L standard flasks in active use at the time we switched from the first to the second URI method allowed us to transfer the calibration from one method to the next. Transferring the calibration from the second URI method to the Princeton method is inherent in the analysis, because both methods compare samples against a standard curve derived from the same primary standards.

[23] Since 1994, when we changed from the first to the second URI procedure, we filled 70-L flasks from four high-pressure cylinders of working standards a total of 16 times at URI and Princeton. From each of these 16 fills, approximately 150 individual aliquots were drawn for analysis. In addition, one fill of standard number 1069 was used as a working standard. With one exception, we assumed that the O_2/N_2 ratio was identical in all 70-L flasks filled from the same high-pressure cylinder (for both working and stability standards). The exception was standard 1514 fill 2, which was clearly offset (by roughly 20 per meg) from other 1514 fills. We then determined six numbers that minimized the squares of the deviations in O_2/N_2 ratios of individual aliquots with respect to the standard curve. These six numbers are the "offsets" of the air in each of the four high-pressure cylinders of working standards (expressed relative to GF 1 in units of per meg); the offset for the anomalous flask, 1514 fill 2; and the distillation correction at URI (0.0226 per meg/aliquot). In addition, we determined the distillation correction at Princeton (0.0097 per meg/aliquot) as follows. Two 70-L glass flasks (Flasks A and B) were filled with gas from the same high-pressure gas cylinder. They were both measured to determine the initial value. Subsequently, aliquots were drawn and measured from Flask A, while Flask B was

stored. After Flask A was analyzed approximately 160 times, both flasks were analyzed to determine the distillation.

[24] One needs to address questions of diffusion of gases through O-rings for standards as well as samples. The large amount of gas suppresses the effects of diffusion. On the basis of our tests as well as those of *Sturm et al.* [2004], diffusion would change the O_2/N_2 ratios of the standards in the 70-L glass flasks by <1 per meg/yr under normal usage. However, the change was much greater in our earliest standards, which were highly depleted and stored for many years. Accordingly, analyses of these standards were rejected after approximately 5 years of storage.

[25] The final step in constructing the standard curve involved deriving the difference between O_2/N_2 ratios of standard fills analyzed at URI against the URI reference gas, and the standard fills analyzed at Princeton against the Princeton reference gas. We determined the Princeton-URI difference in three ways. First, we calculated the mean Princeton–URI difference of all aliquots from the nine 70-L flasks that were analyzed repeatedly at both institutions. The difference was −48 ± 5 per meg (1σ, n = 9 common 70-L flasks); the sign indicates that relative to the reference gas, the numbers at URI were higher than the numbers at Princeton. Second, we limited this comparison to aliquots analyzed during the final 5 months that the URI lab was active, and the first 5 months that the Princeton lab was active. The Princeton-URI difference was then −44 ± 3 per meg (1σ, n = 9 flasks). Finally, we calculated average O_2/N_2 ratios for all aliquots filled from a given high-pressure cylinder at Princeton, and compared these numbers with comparable averages for standards analyzed at URI. The mean difference between the averages for flasks filled at Princeton from those at URI was −42 ± 2 per meg. For constructing the standard curve, we adopt a value of −48 per meg, the result of the largest data set. This number provides continuity between URI and Princeton, but it does not enter into the calculation of sample O_2/N_2 values. These depend only on the difference in O_2/N_2 ratios of samples from standards measured contemporaneously against the same reference gas.

[26] The entire standard curve is shown in Figure 2. The points represent individual aliquots, and the line represents the standard curve as derived using LOESS [*Cleveland and Devlin*, 1988]. Fitting terms for LOESS were f = 0.2, N = 5, δ = 0. The key term is f, which determines the extent of smoothing. We chose a value of 0.2, which corresponds to smoothing over about 70 individual standard analyses, and is a good compromise between using a large number of standard data for computing sample ratios, and a short enough interval to capture variability in the standard curve. The standard deviation of individual aliquots from the curve is ±7 per meg for URI the period, and ±4 per meg for the Princeton period. The reader will note that the standard curve sometimes shows rapid variations where it may be more uncertain. In general, however, few samples were analyzed at times when the standard curve was unstable. The sharp excursion in the second half of 1996 was not associated with any change in analytical methods.

[27] The derivation of the standard curve assumes that all fills from a given high-pressure cylinder start with the same O_2/N_2 ratio. In practice, we recognize that there is some variability: standard flasks are not filled perfectly reproducibly. We can assess this variability as follows. The standard curve is determined by fitting data from all working standard flasks that are active. Typically, there are five active flasks, one for each working standard cylinder, and a flask containing a prior fill that has not yet been retired. Hence each standard fill makes a small contribution (∼20%) to the contemporaneous part of the standard curve. We calculated the mean deviation for each of our 18 working standard fills (excluding the single fill of 1069 used as a working standard, and 1514f2). The standard deviation of the mean of a single fill from all fills from the same high-pressure cylinder is 1.4 per meg (n = 15 fills). This number provides a measure of variability in initial O_2/N_2 of 70-L flasks filled from a given standard cylinder. The worst case was 2706 fill 2, which differed from the mean offset of fills for tank 2706 by 4 per meg. At any one time, the standard curve is calculated by averaging O_2/N_2 ratios from four or more flasks, and the standard error in the standard curve due to errors in filling 70-L flasks is thus less than 1 per meg.

[28] O_2/N_2 ratios of stability standards are corrected for distillation and then calculated by subtracting the standard curve from the measured values. If the standard curve truly captures the drift in the analysis system, the O_2/N_2 ratios of individual stability standards calculated in this manner should be constant over time. One measure of accuracy in the standard curve comes from the variability in O_2/N_2 ratios measured in individual stability standards. For the entire Princeton analysis period (to the first quarter of 2005) the standard deviation from the mean for a given fill ranges from ±3.2 per meg to ±5.9 per meg, with one outlier, which has been analyzed only a small number of times, at ±7.1 per meg. These numbers are based on 1212 individual analyses of 11 fills, with 28 highly anomalous results excluded from the calculations. We also tested for long term drift in the standard curve by subtracting the mean from the O_2/N_2 ratios measured for individual aliquots, and plotting the mean versus time. Because the actual O_2/N_2 ratio of the individual stability standard fills is constant with time, any trend in the residuals reflects drift in the standard curve. The slopes of best-fit lines correspond to standard curve drifts of −0.23 ± 0.24 (s. e.) per meg yr^{-1}. This rate corresponds to an error of 0.1 ± 0.1 Gt C yr^{-1} in partitioning CO_2 sequestration between land and ocean.

2.4. Methods of Sample Analysis

[29] The second URI method, and the Princeton method that followed, were designed to allow analysis of 500–1000 or more sample flasks per year, with extensive standardization and high precision. To achieve these goals, the methods had the following attributes: automated analyses under computer control using LabVIEW™, the presence of multiple equivalent ports for admitting samples, expansion of samples and reference gases at 1 atm nominal pressure to minimize fractionation, identical processing procedure for all samples, identical processing procedure (to the extent possible) for admitting standards and samples, use of inert vacuum line materials wherever possible, and high precision as a result of long analysis times.
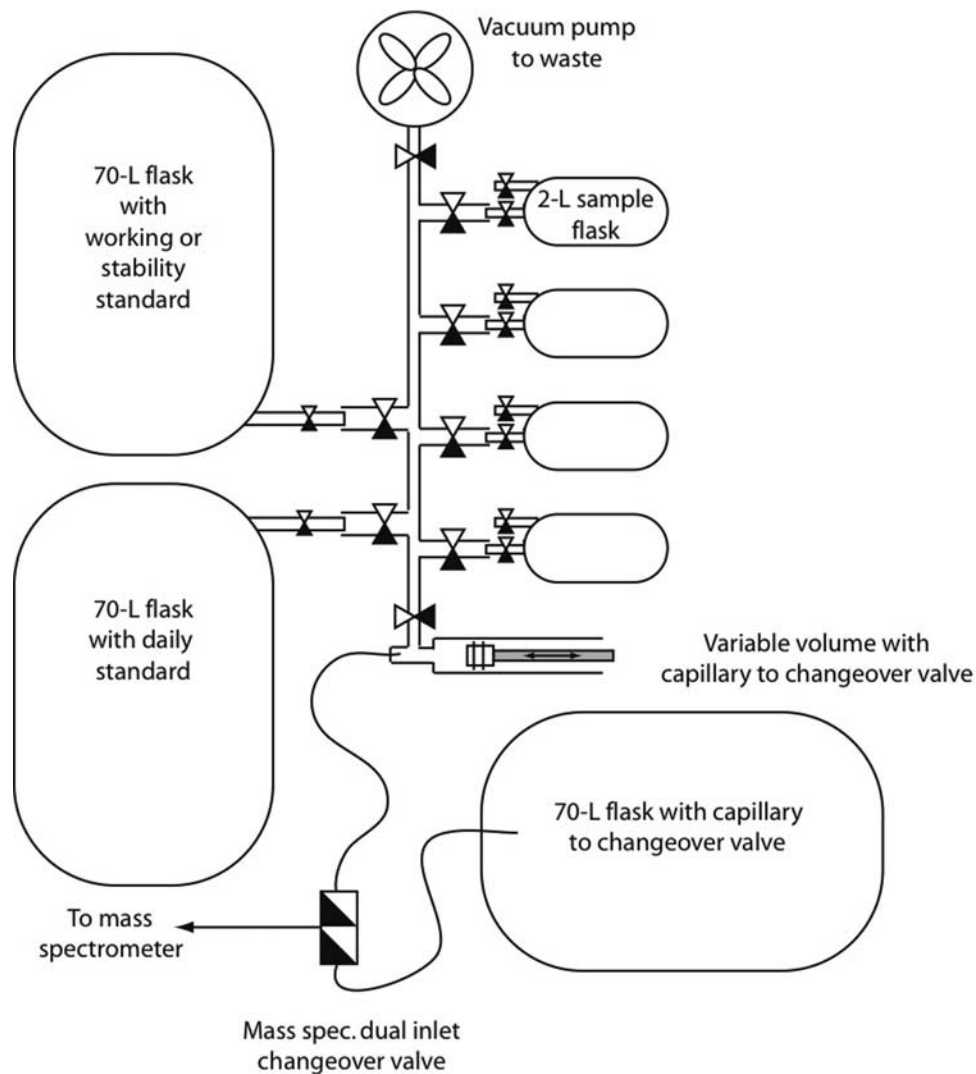
Figure 3.　Schematic of the inlet line used at U. R. I. used in the second U. R. I. method.

[30] Both procedures were set up so that samples and reference gases were analyzed in an automated sequence lasting 14–18 hours that was started in the afternoon and completed early the following morning. Daytime was reserved for replicate analyses of flasks, additional standard analyses, maintenance, etc.

2.4.1. Second URI Method

[31] The glass vacuum line for the second URI method is shown in Figure 3. It included ports for two 70-L standard flasks and four 2-L sample flasks, and valves leading to the pumps and the variable volume. The gas in the 70-L "daily standard flask" was analyzed frequently as a guide to instrumental stability, but was not used for constraining the standard curve. In a normal run, a 70-L standard flask and four sample flasks were attached to the manifold. After evacuation, manual valves of these five flasks were opened, allowing the gas to expand to the automated glass valves of the manifold that then isolated each port. A sample or standard was expanded through the line into the variable volume. At this point it began

flowing through the capillary tube to the sample side of the mass spectrometer's changeover valve. A glass valve was closed to isolate the variable volume, which was a glass cylinder with a moveable aluminum piston sealed by two O-rings. This volume was adjusted by moving the piston with a stepper motor to balance ion currents on sample and reference sides. The sample was then analyzed for O_2/N_2 in two blocks, 25 cycles/block. The line was evacuated and the sample was reanalyzed using the identical procedure. Then the next sample or standard was admitted, and so on. The standard was analyzed 3 times in each nightly cycle: before the first sample, before the third sample, and after the fourth sample.

[32] Each measured O_2/N_2 ratio was corrected for the pressure imbalance between sample and reference sides as described earlier. The O_2/N_2 ratios of aliquots after the first were corrected for the (small) change in O_2/N_2 composition as air was drawn from the flask; the correction was of order 1 per meg/aliquot. Samples were analyzed on different ports; in general, no systematic difference in O_2/N_2 ratio

could be detected. At one point, a dirt particle lodged on the O-ring of one of the four automated glass valves used to admit aliquots from a sample flask, causing the O_2/N_2 of this port to be in error, initially by 5.1 ± 0.9 (s.e.) per meg, and later by 9.4 ± 1.5 (s.e.) per meg. We did not change this O-ring as it would have meant disassembling delicate parts of the apparatus. Rather, the appropriate correction was applied.

[33] Air admitted from the standard port expands into the vacuum manifold in a way that is different from air admitted at the sample ports. To evaluate the possibility that gas introduced on the standard port is fractionated differently from gas introduced at the sample ports, we admitted samples from the same bottle on both ports. This experiment was carried out with 5-L flasks of the type used by R. Keeling [*Keeling et al.*, 1998]; these large flasks allowed the analysis of multiple aliquots on both ports. Samples admitted on the sample port had O_2/N_2 = 8.5 ± 0.8 (standard error) per meg higher than those on the standard port. Thus we subtracted 8.5 per meg from all sample values to make sample and reference gases fully comparable.

[34] The standard deviation from the mean O_2/N_2 ratios measured in sequential blocks (of 25 cycles) from the same inlet is ±6.7 per meg (1σ, n = 12,996). In this and some of the following cases, deviations were not normally distributed. We report both the standard deviation and also the deviation from the mean encompassing 68% of the data points (corresponding to 1 sigma for normally distributed errors). Sixty-eight percent of blocks have a deviation from the mean ≤3.1 per meg. The standard deviation from the mean of O_2/N_2 ratios determined with replicate sample inlets (can be up to nine inlets) is ±5.9 per meg (1σ). Sixty-eight percent of replicate inlets have O_2/N_2 ratios that deviate from the mean by ≤2.7 per meg.

[35] O_2/N_2 ratios for replicate flasks are excluded from the concentration record when the flasks differ by >16 per meg. 91 out of 1143 pairs are excluded by this criterion. The standard deviation from the mean of retained values is ±3.1 per meg. Following *Keeling et al.* [1998], we calculate scaled residuals (d_i) according to their equation (5), multiplying deviations from the mean by $(N/(N-1))^{0.5}$, where N represents the number of replicates. Flasks were measured in duplicate, and the scaled residuals are thus ±4.4 per meg.

2.4.2. Princeton Method

[36] The Princeton inlet system (Figure 4) differs from the URI inlet system primarily in the way samples are connected to the inlet line. The Princeton inlet includes a glass manifold with Louwers-Hapert™ valves to vacuum, variable volume, primary or stability standards, working standard, and carousel. The carousel is a translating and rotating ring to which 12 samples can be connected. In the retracted position, the carousel can be rotated so that a flask of choice will, when engaged, mate to the manifold. In the engaged position, the flask is connected to the vacuum manifold by an aluminum transfer tube, and the flask valve handle is connected by a drive shaft to a rotating cog driven by a stepper motor. The latter allows the flask valve to be opened or closed under computer control. One end of the aluminum transfer tube is sealed to the outlet valve of the sample flask with a compression fitting and Viton™ O-ring. The other end has a polished aluminum face, which seals against a Viton™ quad-ring of the vacuum manifold at 30 psi force.

[37] The carousel inlet has three major advantages. First, every sample enters the vacuum manifold in the same geometry. Second, each sample sees the minimum amount of vacuum components (no tubing or O-rings are used to attach and isolate other flasks to a common manifold). Third, the compact geometry reduces thermal gradients in the system, and all gas flow occurs in a horizontal plane, eliminating significant gravitational fractionation.

[38] The protocol for sample analysis is as follows. Twelve samples and a working or stability standard are put in place and allowed to passively reach temperature equilibrium for 1–3 hours. Then each sample is in turn admitted to the mass spectrometer and analyzed, as described earlier, for $N_2/O_2/Ar$ (28/32/40) and $N_2/^{15}N^{14}N/CO_2$ (28/29/44). Then three aliquots of the standard are admitted and analyzed in the identical manner. The next day, a new standard and the same samples are analyzed, each sample being shifted forward by 1 port position on the carousel. Approximately a week later, the replicate flasks are analyzed in the identical manner. They are placed on the carousel in the same sequence but the port positions are shifted by 4 from the initial positions.

[39] A subset of samples is measured on the standard port so that a correction can be made, as in the URI method, for relating O_2/N_2 ratios of samples to standards. During the analysis period for samples reported here, 761 samples were analyzed on the standard port as well as the sample ports. The sample port–standard port difference, averaged over analysis intervals, ranged from 2 to 22 per meg, with values over 14 pertaining to only a small fraction of the analysis period when mass spec stability was poor. Samples are corrected with the appropriate difference given their analysis date.

[40] The analysis protocol gives extensive information about sample port-to-sample port differences in measured O_2/N_2 ratios. External precision, based on a representative subset of replicate analyses of samples from the same flask and carousel port, is ±4.3 per meg (1σ, n = 1296). Sixty-eight percent of replicate analyses lie within 2.8 per meg of the mean. Systematic port-to-port differences in O_2/N_2 for the same flask are up to 2 per meg. No corrections were made for these differences, which tend to cancel given that flasks and their replicates are analyzed on different ports. Data from 64 out of 731 pairs of flasks were rejected from the six sites reported on in this paper because flask means differed by >16 per meg. Precision (standard deviation from the mean) for remaining replicate flasks was ±3.3 per meg. Again the flasks were measured in duplicate, and the scaled deviation is ±4.7 per meg.

2.5. CO_2 Measurements

[41] After O_2/N_2 analysis, the flasks were sent to NOAA/ CMDL for CO_2 measurements. The measurements were
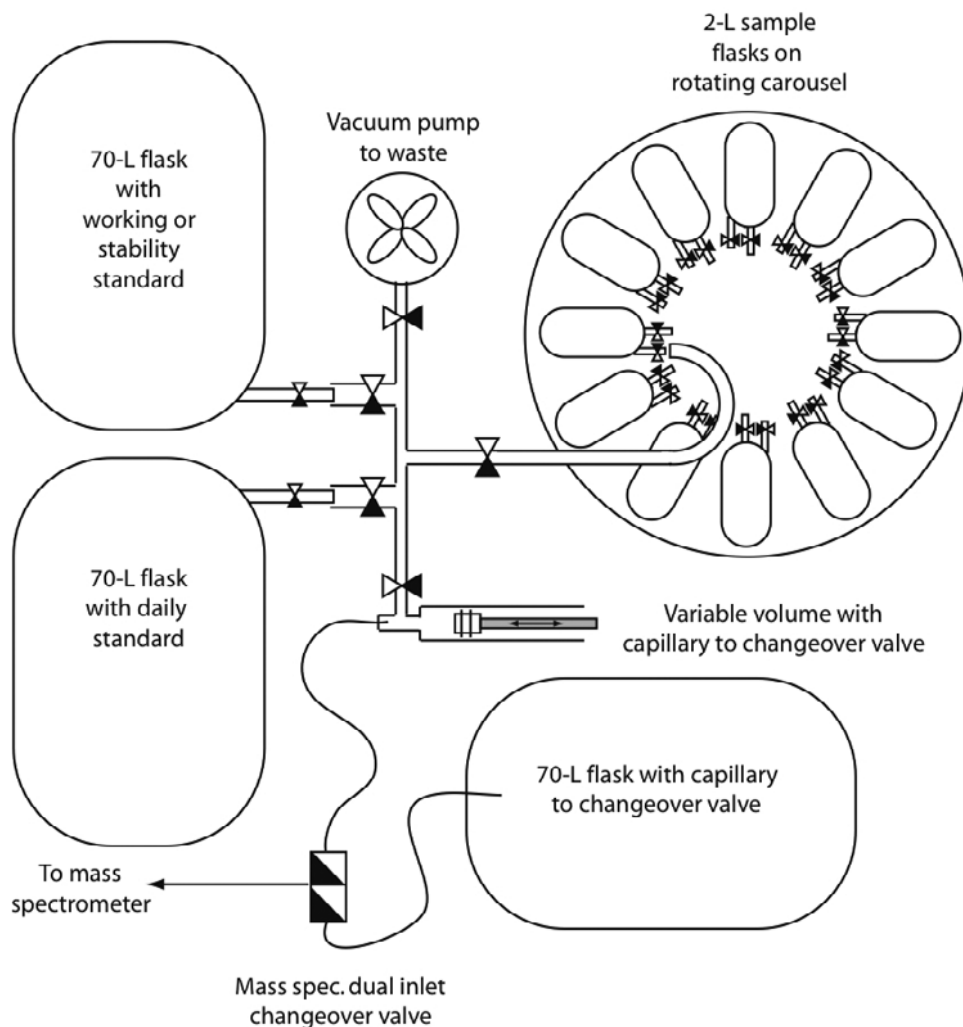
Figure 4.   Schematic of the inlet line used at Princeton.

made by nondispersive infrared absorption, using the method described by *Conway et al.* [1994]. CO_2 concentrations measured on these samples generally agree with values measured on samples of the CMDL flask network to within ±0.2 ppm.

2.6. Rejection Criteria

[42] In addition to the requirement that O_2/N_2 replicates agree within ±8 per meg, we rejected data for four additional reasons. First, we rejected samples that, on visual inspection, fell far from the envelope of O_2/N_2 vs. time, as defined by the bulk of the data. Included in this group were samples falling outside the main envelope by hundreds of per meg, and five Cape Grim points that were among the first group of samples analyzed at Princeton. Including these latter samples would have yielded a large (∼40 per meg) secondary O_2/N_2 maximum in austral fall of 1998, a feature completely absent during every other year. Second, we calculated the standard deviations of residuals from the smoothed curve of O_2/N_2 vs. time, using the protocol of *Thoning et al.* [1989]. We rejected flask pairs falling off the smooth curve by more than

4 standard deviations, and repeated this procedure until no points fell more than 4 standard deviations from the mean. A total of 72 samples were rejected by these criteria. Several factors would have lead to anomalous data: insufficient drying of the samples, undue influence on O_2/N_2 ratios by the local vegetation, errors in sample collection, and unrecognized transient problems with the mass spec inlet line.

[43] Third, we rejected a full year's data from Syowa (mid-January 1998 to mid-January 1999). This interval comprises a unit in that it precisely covers one shipping period and winter-over period at that station. The samples appear anomalous for the following three reasons. O_2/N_2 values, which are close to Cape Grim values during all other years, are systematically higher during the 1998–1999 year by about 20 per meg. CO_2 values at Syowa, measured in the O_2/N_2 samples, are higher than Cape Grim values, by about 0.5 ppm, throughout the year. We occasionally observe higher CO_2 values at Syowa, but, in other years, the discrepancy never lasts more than about 6 months. Finally, CO_2 concentrations measured in flasks of the NOAA CMDL program are
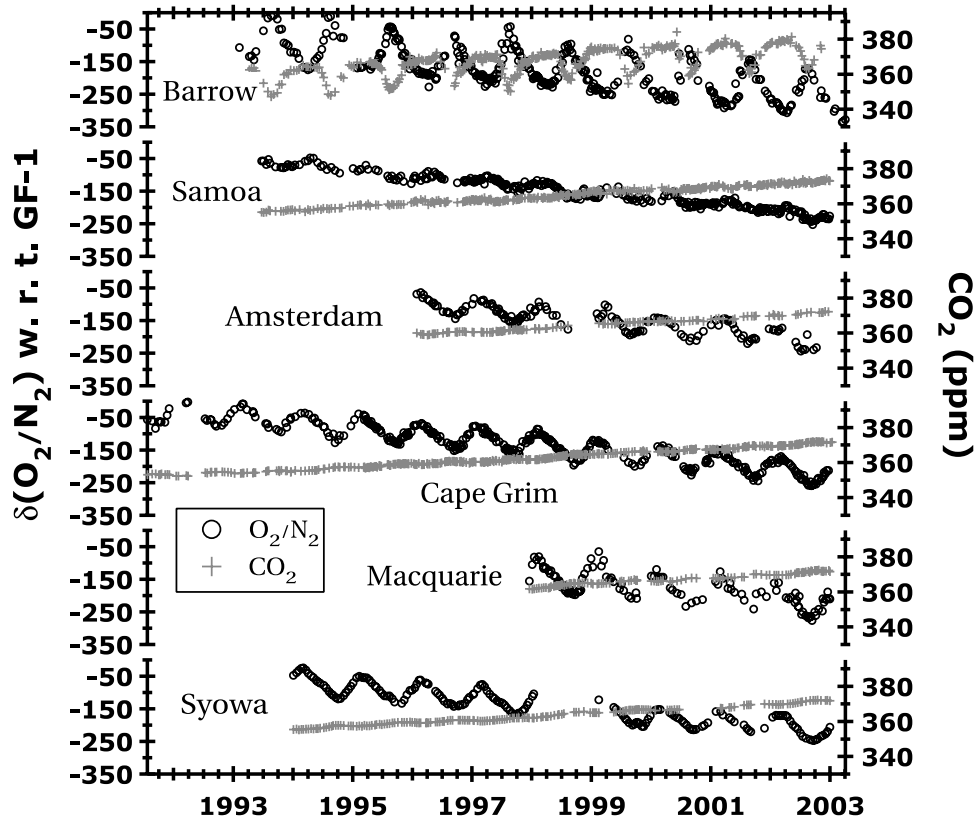
Figure 5. O_2/N_2 and CO_2 records of this study.

anomalously high, and anomalously noisy, during this period (ftp.cmdl.noaa.gov).

[44] Finally, certain CO_2 data are rejected according to criteria of *Conway et al.* [1994].

3. Results

[45] O_2/N_2 and CO_2 measured at our six sampling stations are shown in Figure 5. The data show the expected trends [e.g., *Keeling and Shertz*, 1992; *Keeling et al.*, 1998; *Battle et al.*, 2000]: CO_2 concentrations increase with time, while O_2/N_2 ratios decrease. The seasonal cycles of O_2/N_2 and CO_2 are out of phase. The amplitude of O_2/N_2 cycles is larger than that of CO_2: amplitudes due to land sources are comparable, but the seasonal source of the ocean is much greater for O_2 than for CO_2.

3.1. Equations for Calculating Land and Ocean Carbon Sequestration

[46] Data from Barrow, Cape Grim, and Samoa are used to partition anthropogenic CO_2 uptake by the land biosphere and the ocean. These sites have the longest records, greatest sampling frequency (weekly over much of the records), and fewest gaps. Sampling began in spring 1991 at Cape Grim; in February 1993 at Barrow; and in June 1993 at Samoa. Hence, in order to have complete data sets, we restrict the calculation of land and ocean carbon uptake to the period from 1994 to 2002.

[47] Global CO_2 concentrations and O_2/N_2 ratios were calculated by simple averaging of values at Barrow, Samoa, and Cape Grim,

$$(CO_2)_{global} = \left[(CO_2)_{BRW} + (CO_2)_{CGT} + (CO_2)_{SMO}\right]/3 \quad (2)$$

$$\delta(O_2/N_2)_{global} = \left[\delta(O_2/N_2)_{BRW} + \delta(O_2/N_2)_{CGT} + \delta(O_2/N_2)_{SMO}\right]/3 \quad (3)$$

[48] For our purposes, it is important that these values accurately reflect annual changes in the gas properties, rather than that they give accurate measures of the global average at any one time.

[49] The atmospheric mass balance of CO_2 and O_2 are expressed as follows [*Battle et al.*, 2000]:

$$\frac{d(CO_2)}{dt} = -\beta \times (f_{fuel} + f_{cement} + f_{land} + f_{ocean}) \quad (4)$$

$$\frac{d(O_2/N_2)}{dt} = \gamma \times \beta \times (\alpha_{fuel}f_{fuel} + \alpha_{bio}f_{land}). \quad (5)$$

Units of CO_2 are ppm, O_2/N_2 are per meg, and f (flux) terms are Gt C yr^{-1}. Here α is dimensionless, β has units of ppm/Gt, and γ of per meg/ppm. All flux terms are negative for flux to the atmosphere (i.e., positive fluxes

Table 3. Conversion Factors and Other Terms for Calculating the Anthropogenic Mass Balance

Symbol	Description	Number
β	Gt C to ppm CO_2	0.471
γ	ppm O_2 to per meg $\delta(O_2/N_2)$	4.8
α_{fuel}	mean $\Delta O_2/\Delta CO_2$ during combustion	−1.45
α_{bio}	mean $\Delta O_2/\Delta CO_2$ during photosynthesis/respiration	−1.1

correspond to net CO_2 uptake by the oceans and the land biosphere). The f_{fuel} and f_{cement} are sources of CO_2 from fossil fuel burning and cement manufacturing, respectively. The f_{ocean} and f_{land} are the ocean and terrestrial biosphere sinks of CO_2. α_{fuel} is the average O_2:C molar exchange ratio for fossil fuels burned during the period of O_2 and CO_2 measurement, and α_{bio} is the O_2:C molar exchange ratio for photosynthesis and respiration. The β converts Gt C to ppm CO_2, and γ converts ppm to per meg. Values for β, γ, α_{bio}, and α_{fuel} are summarized in Table 3. Equations (4) and (5) assume that the annually averaged O_2 inventory of the oceans is constant. In fact, there is strong evidence that this inventory has been decreasing, with an associated flux of O_2 from ocean to atmosphere. We first calculate sequestration neglecting this change, then make an appropriate correction for the changing ocean O_2 inventory.

[50] O_2 consumed by fossil fuel burning is calculated from fossil fuel combustion estimates of *Marland et al.* [2003], assuming that utilization of all sources rose by 1% in 2001 and 2002 (years for which data are not yet available); α_{fuel} was determined from the utilization-weighted average $\Delta O_2/\Delta CO_2$ for natural gas (−1.95), crude oil (−1.44), solid carbon (−1.17), and gas flaring (1.98) [*Keeling*, 1988]. For the total fossil fuel combusted from 1994–2002, α_F was −1.45. Solving equations (4) and (5) for f_{land} and f_{ocean} in terms of measured and known quantities, we obtain

$$f_{land} = -\frac{\alpha_{fuel}}{\alpha_{bio}} f_{fuel} + \frac{1}{\beta\gamma\alpha_{bio}} \frac{d(O_2/N_2)}{dt} \quad (6)$$

$$f_{ocean} = -\frac{\alpha_{bio} - \alpha_{fuel}}{\alpha_{bio}} f_{fuel} - f_{cement} - \frac{d(CO_2)/dt}{\beta}$$
$$- \frac{1}{\beta\gamma\alpha_{bio}} \frac{d(O_2/N_2)}{dt}. \quad (7)$$

[51] Atmospheric potential oxygen, APO, which is unaffected by exchange of CO_2 and O_2 between the atmosphere and the land biosphere [*Stephens et al.*, 1998], is defined as

$$APO = O_2/N_2 + \gamma\alpha_{bio}CO_2. \quad (8)$$

Hence, after combining and rearranging equations (4), (5) and (8), we obtain

$$\frac{dAPO}{dt} = \gamma \times \beta \times \alpha_{bio} \left(\frac{(\alpha_{fuel} - \alpha_{bio})}{\alpha_{bio}} f_{fuel} - f_{cement} - f_{ocean} \right). \quad (9)$$

Solving equation (9) for f_{ocean} in terms of measured or known quantities, we obtain

$$f_{ocean} = -\frac{\alpha_{bio} - \alpha_{fuel}}{\alpha_{bio}} f_{fuel} - f_{cement} - \frac{1}{\beta\gamma\alpha_{bio}} \frac{d(APO)}{dt}. \quad (10)$$

Then

$$f_{land} = -f_{fuel} - f_{cement} - f_{ocean} - \frac{1}{\beta} \frac{dCO_2}{dt}. \quad (11)$$

3.2. Partitioning of CO_2 Sequestration, 1994–2002

[52] Our observations begin in 1991 at Cape Grim and in 1993 at Samoa and Barrow. We base our calculation of sequestration on these three sites because, elsewhere, observations commence more recently and sampling density is lower. We make calculations for the period mid-1993 to mid-2002 based on data from Cape Grim only, and between mid-1994 and mid-2002 based on data from Cape Grim, Samoa, and Barrow. We emphasize that the products of these calculations are net global fluxes of CO_2 between the land biosphere and the atmosphere, or between the oceans and the atmosphere.

[53] Between mid-1993 and mid-2002, 56.3 Gt C was released to the atmosphere from fossil fuel combustion and another 1.9 from cement manufacture [*Marland et al.*, 2003]. At the same time, the atmospheric CO_2 concentration, as represented by data from CGO, rose by 15.3 ppm (32.5 Gt C). Therefore the total carbon sink averaged 2.9 Gt C yr^{-1} over the study period. Ocean and land uptake rates calculated from our data are 1.8 and 1.1 Gt C yr^{-1}, respectively. From mid-1994 to mid-2002, we can make this calculation by averaging data from Barrow, Cape Grim, and Samoa. For this period, ocean and land CO_2 uptake average 1.4 and 1.3 Gt C yr^{-1}, respectively. (Corrected for ocean O_2 outgassing, as explained below, we calculate ocean and land CO_2 sequestration rates, respectively, as 2.1 and 0.8 Gt C yr^{-1} from 1993–2002, and 1.7 and 1.0 Gt C yr^{-1} from 1994–2002.)

[54] In making these estimates, we calculate CO_2 and APO values for individual flask samples using equation (8). We then calculate deseasonalized CO_2 and APO values for BRW, SMO and CGO, with 620-day smoothing, using the algorithm of *Thoning et al.* [1989] (hereinafter referred to as CCGVu). This level of smoothing is roughly equivalent to a 1-year running average. From these curves, we calculate annually averaged values at BRW, SMO, and CGO, and, for 1994–2002, calculate the yearly global average of the three sites. Using these values, we calculate sequestration rates from equations (10) and (11). Fossil fuel combustion rates come from *Marland et al.* [2003]; other terms are summarized in Table 3.

[55] These numbers need to be modified to account for the transfer of O_2 from ocean to atmosphere, and it is to this subject that we turn next. Global warming is likely to lead to some transfer of O_2 from the ocean to the atmosphere. Such a change would lead to an increase in the atmospheric O_2 inventory, which we would incorrectly attribute to a carbon flux to the land biosphere. The possibility of an ocean efflux

arises for two basic reasons. First, the ocean is warming, lowering solubilities and causing degassing. Since O_2 is more soluble than N_2, the O_2/N_2 ratio of air rises. The rate may be estimated from the increased heat load of the oceans [*Levitus et al.*, 2000], although one also needs to estimate the temperature distribution of the warming waters.

[56] Second, the ocean carbon cycle may be changing in a way that induces transfer of O_2 to the atmosphere. Increased upper ocean stratification, expected given upper ocean warming and high-latitude freshening, will lead to increased utilization of nutrients. This change, in turn, increases the export of organic carbon to depth; it decreases the fraction of "preformed" nutrients that go unutilized in surface water and passively sink during subduction [e.g., *Keeling and Garcia*, 2002]. Furthermore, an increase in the C/nutrient ratio of organic matter in oligotrophic waters would induce O_2 transfer to the atmosphere. Such a change has been invoked to explain decreasing $[O_2]$ in the upper thermocline of the subtropical North Pacific [*Emerson et al.*, 2001].

[57] A considerable effort has gone into assessing the rate of ocean O_2 degassing. We may divide the work into three approaches: local, large-scale and model studies. First, in careful local studies, *Emerson et al.* [2001] document a large decrease in dissolved O_2 in thermocline waters from $25°–45°$ N along a meridional line through the subtropical North Pacific gyre (described above), and *Shaffer et al.* [2000] find decreasing $[O_2]$ in waters off the Chilean coast. *Andreev and Watanabe* [2002] conclude that $[O_2]$ is rising in waters of the subpolar North Pacific; however, the trend may disappear if one removes the decadal cyclicity that the authors link to the North Pacific Index. Second, three large-scale (basin-wide or global) studies demonstrate little change in O_2 inventories during recent decades, and no evidence for systematic decreases in ocean $[O_2]$ [*Pahlow and Riebesell*, 2000; *Bindoff and McDougall*, 2000; *Keller et al.*, 2002]. On the other hand, *Matear et al.* [2000] analyzed a limited data set and deduced significant O_2 outgassing in a $30°$ zonal sector of the Southern Ocean. This result agrees with their model predictions of increased Southern Ocean stratification, diminished ventilation, and hence decreasing dissolved $[O_2]$ in seawater. Third, three additional modeling studies [*Sarmiento et al.*, 1998; *Plattner et al.*, 2002; *Bopp et al.*, 2002] and a data analysis paper [*Keeling and Garcia*, 2002] estimate the rate of O_2 outgassing by empiricism and deduction. Each estimates an O_2 flux to the atmosphere of 5–6 nmol O_2/Joule of ocean warming (mainly due to a changing carbon cycle), and calculates the recent O_2 efflux from the heat flux of *Levitus et al.* [2000]. Their calculated O_2 fluxes differ by a factor of 2 (corresponding to a sequestration correction of 0.3–0.6 Gt C yr^{-1}) due largely to differences in adopted values of the heat flux.

[58] We have adopted the lower estimates (0.3 Gt C yr^{-1}) for four reasons. First, existing basin-scale studies do not support large outgassing except in the Southern Ocean, where few data have been analyzed. Second, biogeochemical outgassing is likely to be small during the early part of the anthropogenic transient, because much of the heat storage is in the upper water column [*Levitus et al.*, 2000]. Since these waters are largely nutrient-free ($O_2^* \sim$

$[O_2]_{sat}$) in the analysis of *Keeling and Garcia* [2002], warming cannot induce much increase in net euphotic zone nutrient utilization and biogeochemical O_2 outgassing. Third, most whole-ocean warming from 1990–1995 takes place in the first year and a half of the decade [*Levitus et al.*, 2000]. This 1.5-year period, included in the Bopp analysis, predates our study period. Finally, Keeling and Garcia based their estimate of ocean warming on the heat content record of the upper 300 m, which extends to 1998. Through extrapolation, they account for warming below 300 m (climatologically about 25% of the total), and their correction is more appropriate to our record.

[59] Ultimately, the current uncertainty in the O_2 outgassing correction is less important than the ability of the community to narrow the uncertainty in the coming years. Current O_2-based estimates of land and ocean carbon sequestration have an uncertainty of order ± 0.3 Gt C $yr^{-1}yr^{-1}$ due to uncertainty about the rate of ocean outgassing. We expect that the uncertainty will be narrowed by the analysis of historical ocean O_2 concentration data, supplemented by the ongoing CLIVAR Repeat Hydrography Program, and by studies with models carefully evaluated in the context of these extensive data sets.

[60] Invoking the correction of 0.3 Gt C yr^{-1} raises calculated ocean uptake for 1993–2002 to 2.1 Gt C yr^{-1} and lowers land uptake to 0.8. For the 1994–2002 period, the comparable numbers are 1.7 and 1.0 Gt C yr^{-1}, respectively. If one used the modeled corrections of 0.60 Gt C yr^{-1}, one would estimate ocean uptake at 2.0–2.4 Gt C yr^{-1} (starting in 1993 and 1994, respectively), and net land uptake as 0.5–0.7 Gt C yr^{-1}. The latter result still implies a large land sink, since terrestrial deforestation gives regional sources that sum to order 1 Gt C yr^{-1} [*Schimel et al.*, 2001].

[61] Uncertainties in these numbers arise from analytical errors, uncertainties in the change in atmospheric O_2 and CO_2 due to limited sampling, uncertainties in air-sea O_2 exchange, and uncertainties in fossil fuel combustion rates and stoichiometry. We consider that the analytical errors are negligible with respect to calculations of carbon sequestration over the length of the record, because of the absence of detectable drift in stability standards and the large number of samples analyzed. For reference, O_2/N_2 drift of 0.5 per meg/year (2 σ of the stability standard drift) corresponds to an error in carbon partitioning of 0.2 Gt C yr^{-1} in the land and ocean reservoirs. We estimate the error in sampling the atmosphere from the sites having the poorest agreement in APO changes from 1994–2002. These are Barrow and Cape Grim, which differ by ± 3 per meg over the length of the record. This difference translates to an uncertainty in partitioning of about 0.1 Gt C yr^{-1}. We estimate the uncertainty in combustion rate as ± 0.4 Gt C yr^{-1} [*Keeling and Shertz*, 1992]; this term leads to an uncertainty in ocean uptake of ± 0.1 Gt C yr^{-1}, and land C uptake of ± 0.4 Gt C yr^{-1}. (Equation (10) shows that uncertainty due to combustion is smaller for ocean sequestration because it enters only as the difference between land biosphere and fossil fuel stoichiometry.) Finally, we estimate the uncertainty in α_{bio} as ± 0.05 (estimated from results of *Severinghaus*

Table 4. Oceanic CO$_2$ Uptake During the 1990s Calculated in This Study and Other Recent Work[a]

Method	Period	Ocean Net	Ocean Fossil
O$_2$/N$_2$ (CGO only: this paper)	1993–2002		**2.1 ± 0.5**
O$_2$/N$_2$ (BRW, CGO, SMO: this paper)	1994–2002		**1.7 ± 0.5**
O$_2$/N$_2$ (*Manning* [2001])	1990–2000		**1.7 ± 0.5**
Sea surface pCO$_2$ (*Takahashi et al.* [2002])	1995	**2.2 ± 0.2**	2.8
Atmospheric CO$_2$ inversion (*Gurney et al.* [2003])	1992–1996	**1.5 ± 1.1**	2.1
Atmospheric CO$_2$ inversion (*Rodenbeck et al.* [2003])	1990–1999	**1.4 ± 0.3**	2.0
Ocean CO$_2$ inventory (*McNeil et al.* [2003])	1990s		≤**2.0 ± 0.4**
Ocean GCMs (13 models; *McNeil et al.* [2003])	1990s		2.2–2.8

[a]Units are Gt C yr^{-1}. Values are reported as ocean net CO$_2$ uptake and ocean uptake of fossil fuel CO$_2$. Fossil uptake is greater than net uptake by 0.6 Gt C yr^{-1} owing to oxidation of riverine organic CO$_2$ followed by CO$_2$ outgassing, as well as by precipitation of CaCO$_3$, also followed by CO$_2$ outgassing [*Sarmiento and Sundquist*, 1992; *Ludwig and Probst*, 1996]. Estimates based on O$_2$/N$_2$ ratios, from *Manning* [2001] (based on measurements in the laboratory of R. F. Keeling) and from this study, include an ocean outgassing correction of 0.3 Gt C yr^{-1}. The constrained values are shown in bold print, and derived values in plain print.

[1995]). The corresponding uncertainty in partitioning is ±0.3 Gt C yr^{-1}. To these numbers, we must add an additional uncertainty of ±0.3 Gt C yr^{-1} due to the ocean O$_2$ imbalance. It is difficult to know how to propagate these uncertainties. We recognize that they are not normally distributed but nevertheless choose to add them quadratically, since they are independent, and unlikely to all trend in the same direction. The resulting uncertainty is ±0.5 Gt C yr^{-1} for ocean sequestration and ±0.6 Gt C yr^{-1} for land sequestration.

[62] Our computed carbon sequestration rates are compared with other recent estimates of ocean uptake in Table 4. With respect to ocean uptake, O$_2$/N$_2$ based studies such as ours access rates of fossil fuel CO$_2$ uptake by the oceans, whereas studies of air-sea pCO$_2$ disequilibrium and atmospheric inversions access net oceanic CO$_2$ uptake. The numbers differ by the amount of ocean degassing due to oxidation in the oceans of terrestrial organic matter, and precipitation of CaCO$_3$ [*Sarmiento and Sundquist*, 1992]. These two fluxes sum to 0.6 Gt C yr^{-1}, and we correct ?pCO$_2$ and inversion flux estimates for these terms. Tabulated rates of fossil fuel CO$_2$ uptake by the ocean (taking inversion estimates as a single number) then fall within the range 2.2 ± 0.6 Gt C yr^{-1}. Some variability may be due to the fact that different approaches characterize different times; we cannot now say. Estimates based on O$_2$/N$_2$ data continue to be near the lower end of the range.

3.3. Interannual Variability in Land and Ocean CO$_2$ Uptake

[63] Equations (10) and (11) show how calculated values of f_{ocean} and f_{land} depend on fossil CO$_2$ sources, stoichiometric terms, and rates of change of O$_2$/N$_2$, CO$_2$, and APO. Over the length of the O$_2$/N$_2$ record, fossil terms and stoichiometric terms change slowly, and calculated rates of sequestration change mainly because of variations in rates of change of O$_2$/N$_2$ and APO (Figure 6). Land CO$_2$ sequestration can be calculated from the rate of change of O$_2$/N$_2$ alone (equation (6)), and decreases as d(O$_2$/N$_2$)/dt becomes more negative. Ocean CO$_2$ sequestration can be calculated from the rate of change of APO alone (equation (10)), and increases as d(APO)/dt becomes more negative. (We note that these calculations can be made either by using values of APO versus time calculated by CCGVu, as is done

here, or by adding values of O$_2$/N$_2$ and CO$_2$ calculated by CCGVu. The results are not perfectly equivalent because of details of the curve fits. Differences in ocean sequestration calculated by the two methods are far smaller than the variation of the rates calculated from fitting APO vs. time, and are not considered further.)

[64] We calculate rates of change in O$_2$/N$_2$ and APO from the trend in deseasonalized values fitted to observations using the CCGVu program [*Thoning et al.*, 1989] with a 620-day smoothing period, corresponding roughly to 1-year smoothing. As one estimate of the analytical error, we analyze data for the period from 999 to 2005 from three stability standards (1069, 1510, and 2619) in the same way
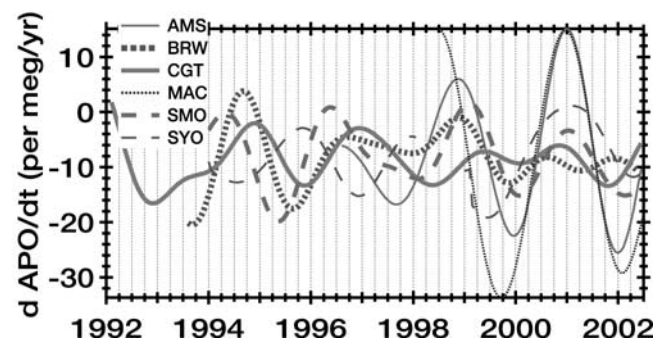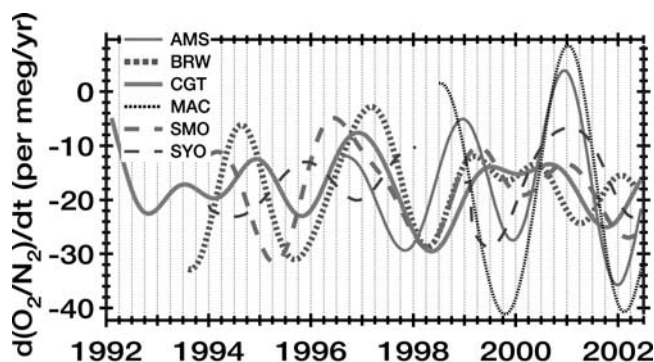
Figure 6. Rates of change of O$_2$/N$_2$ (top) and APO (bottom) in smoothed deseasonalized records from our study sites. See color version of this figure at back of this issue.

as our samples. The largest rate of inferred O_2/N_2 variability is about 1 per meg yr^{-1}, corresponding to an error in land or ocean sequestration of about 0.4 per meg yr^{-1}.

[65] In examining the O_2/N_2 and APO records, we divide our sites into two groups. Cape Grim, Barrow, and Samoa, are our best constrained sites, with the longest records, fewest gaps, and highest sampling resolution (nominally weekly). We focus primarily on these three sites. Fluxes derived from the observations at Amsterdam, Macquarie and Syowa are less well constrained, because records are shorter, gaps are present, and collection frequency is lower.

[66] The pattern of O_2/N_2 variations is similar at each of the three primary sites, and the amplitude of the variations is coherent. These attributes give us confidence that the variability does not originate with artifacts of sampling, which would cause each site to vary independently. In principle, the variability could be analytical: samples from these sites collected at the same time were analyzed at about the same time. However this source would require drift in the standard curve of 5–10 per meg/year, sustained over a period of a year or so. Such drift is unlikely given the absence of detectable drift in the stability standards, and the excellent agreement of O_2/N_2 ratios measured for samples analyzed in our lab as well as the lab of R. Keeling [*Manning*, 2001]. Most of this variability is likely real. As discussed below, it reflects the combined variations of CO_2 uptake by the land biosphere, and interannual imbalances of the ocean O_2 inventory.

[67] The O_2/N_2 variations are highly correlated and in phase between BRW and CGO. However, variations at Samoa lead variations at the other two sites by up to 4 months (Figure 6). These results suggest that the land sequestration and ocean imbalance signals may originate mainly in the tropics. However, a firm conclusion is premature, because the influences on O_2/N_2 at Samoa are complex [*Manning et al.*, 2003], and because the Samoa lead is clearly absent for the latter part of the record (Figure 6).

[68] The variability in the rate of O_2/N_2 decrease at our secondary sites is puzzling. The variations at SYO and MAC are larger than at our primary sites, and the excursions are not coincident with those at the primary sites. Variations at Syowa and Amsterdam coincide, and may represent an Indian Ocean signal. Our two closest sites, MAC and CGO, do not share much variability. MAC is at 55°S latitude, in the middle of the Southern Ocean, and may be too strongly affected by local and synoptic scale variability to record regional trends. A future paper will deal with interannual variability at CGO, SYO, MAC, and AMS.

[69] The amplitude of the APO variations is generally smaller than those of O_2/N_2 (Figure 6). This characteristic reflects the fact that APO excludes variability in the land biosphere. Unlike O_2/N_2 variations, APO variations are not highly coherent at the major sites. In a lagged correlation analysis, Barrow leads Cape Grim by about 0.5 years, and the correlation coefficient is 0.57 at this phase (so that 34% of the filtered variance is shared). Shared variance is lower between SMO and the other two sites. Nevertheless, we argue that there are strong similarities in the APO records from BRW, SMO, and CGO. Visual inspection of the record shows that each of the three major sites has the same number of cycles between 1994 and 2002, although maxima and minima are offset by up to 6 months. As is the case with O_2/N_2, APO variability at the secondary sites is greater than at the major sites, and variability is similar at Syowa and Amsterdam. Macquarie is distinct, and in fact variations in deseasonalized APO at Macquarie appear to be out of phase with Cape Grim for much of the record.

[70] If we assume all oceanic O_2/N_2 fluxes are tied to carbon fluxes, we can use equation (10), together with combustion rates and the atmospheric mass balance, to compute variations in land and ocean fossil fuel CO_2 sequestration rates since 1994. Such calculations do not correct for ocean O_2 outgassing. Land and ocean sequestration rates are plotted versus time in Figure 7, and compared with total sequestration rates. The latter are constrained by fossil fuel combustion rates and the atmospheric CO_2 increase, both of which are well known. The most compelling result is that CO_2 sequestration rates by the land biosphere covary closely with total sequestration rates from 1995–2001, except that the decrease in land sequestration in 1999 leads total sequestration by about 6 months. The most dramatic climate event during this period, the 1997–1998 El Niño, was accompanied by a rapid CO_2 growth rate. Our data indicate that rapid CO_2 growth was due to a diminished land sink (or small land source). This work thus supports many previous studies linking rapid atmospheric CO_2 growth rates with diminished land carbon uptake during El Niño events [e.g., *Keeling et al.*, 1989; *Clark et al.*, 2003; *Nemani et al.*, 2003; *Schaefer et al.*, 2002; *Reichenau and Esser*, 2003]. The primary mechanism is now thought to be increased aridity and biomass burning in tropical areas during El Niño events [*Langenfelds et al.*, 2002; *van der Werf et al.*, 2004].

[71] Another striking feature of the interannual variability is its large magnitude in the oceans, and the anticorrelation of land and ocean variability during most of the record. During an El Niño event, both features are expected. Ocean CO_2 sequestration is enhanced because warming of the equatorial Pacific suppresses upwelling and the attendant transfer of CO_2 to the regional atmosphere [e.g., *Feely et al.*, 2002]. At the same time, drying of tropical regions leads to a net CO_2 flux from the land biosphere to the atmosphere (citations above).

[72] *Battle et al.* [2000] used O_2/N_2 data (including data presented here for BRW, CGO, and SMO) to estimate land and ocean CO_2 sequestration between 1991 and 1998. They compared their results with sequestration rates inferred from $\delta^{13}C$ of atmospheric CO_2, which constrains these terms because land uptake discriminates strongly against the heavy isotope. Their data treatment differed from ours primarily in that they smoothed with a filter equivalent to producing a 2-year running average, whereas ours corresponds to 1 year. Their records of changing sequestration rates were correspondingly smoother. For the period from the beginning of 1993 to mid-1996, their estimates of variations in land and ocean CO_2 uptake based on O_2/N_2 closely tracked estimates based on $\delta^{13}C$ of CO_2, a result likely to reflect real variability. The longer averaging time will remove some artifacts associated with analytical errors
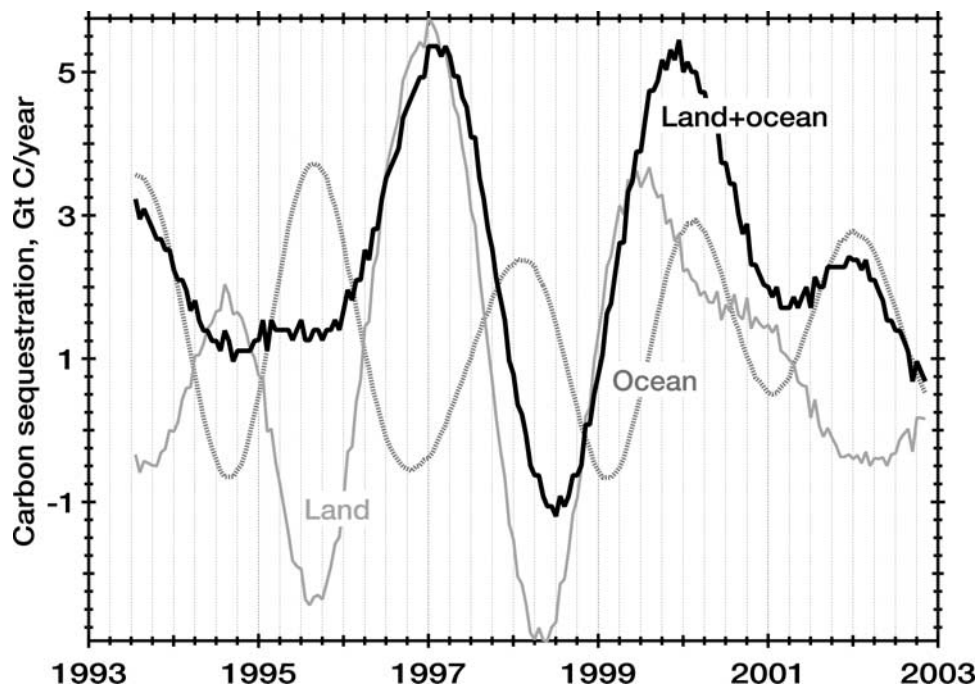
Figure 7. Land and ocean CO_2 sequestration rates calculated from CO_2 and O_2/N_2 data at CGO, SMO, and BRW. See color version of this figure at back of this issue.

and annual changes in air-sea O_2 transfer, but here we restrict the comparison to 1-year smoothing.

[73] At non El Niño times, the balance of evidence suggests that the large ocean amplitude in sequestration rates calculated with 1-year averaging (Figure 7), and ocean-land antiphasing, are artifacts. They may result from analytical error and/or non-zero net O_2 exchange between the oceans and the atmosphere. During these non-El Niño times, there is no known coupling between the oceans and land biosphere that would introduce out-of-phase behavior. Interpretations of the distribution of CO_2 in the atmosphere do not support out-of-phase behavior. For example, *Rodenbeck et al.* [2003] used an inverse approach, together with atmospheric transport based on reanalyzed winds, to calculate land and ocean sequestration rates since 1982. They also summarized earlier results of inverse calculations by *Rayner et al.* [1999] and *Bousquet et al.* [2000]. None of these calculations show as much variability in ocean sequestration rates as our O_2 calculations, nor do they deduce variability that is coherent with our record. The results of *Rodenbeck et al.* [2003] for the period from 1995 to 2001 are based on the largest CO_2 sampling network (i.e., the NOAA Climate Monitoring and Diagnostics Laboratory network) and, therefore, arguably are best constrained. The range of ocean variability computed for this period is 0.9 Gt C yr^{-1}, compared to 3.6 Gt C yr^{-1} in our record.

[74] A number of data analyses and modeling studies suggest that variability in oceanic CO_2 sequestration rates should be much less than we deduce from our O_2/N_2 record, averaged at 1-year periods (Figure 7). *Lee et al.* [1998] estimated the magnitude of interannual variability by relating sea surface CO_2 to sea surface temperature.

They then computed interannual variability of air-sea CO_2 fluxes from variability in winds (NCEP reanalysis: *Kalnay et al.* [1996]) and historical sea surface temperature data. They concluded that interannual variability was less than ±0.2 Gt C yr^{-1} (1σ).

[75] *Le Quéré et al.* [2000, 2003] and *McKinley et al.* [2004] estimated interannual variability in CO_2 sequestration rates using biogeochemical ocean circulation models and surface wind fields to specify sea surface pCO_2 and air-sea exchange rates. They concluded that interannual variability would be of order ±0.4–0.5 Gt C yr^{-1}. Accepting their low model values of interannual CO_2 variability implies an accompanying real world variability in annually averaged air-sea O_2 fluxes, with a magnitude sufficient to account for the large artifactual interannual variability in carbon sequestration that we estimate on the basis of O_2 observations. *McKinley et al.* [2003] used a biogeochemistry ocean GCM to calculate interannual variability of air-sea O_2 fluxes. In their model, this variability is large enough to account for a significant fraction of inferred variability in ocean sequestration.

[76] It remains a concern that the models may underestimate true variability in ocean carbon fluxes. Also relevant here is the fact that there is shared variability in land versus ocean sequestration extending back to 1993, as estimated using highly smoothed records of global $\delta^{13}C$ of CO_2 and O_2/N_2 at Cape Grim [*Battle et al.*, 2000]. Nevertheless, the most likely conclusion at this point is that interannual variability in ocean sequestration rates is significantly less than estimated from atmospheric O_2 data. The assumption that the only imbalance in the ocean O_2 inventory comes from slow, continuous, O_2 outgassing appears to be invalid. The origin of the ocean O_2 imbalance, and its relationship, if

any, with other modes of interannual variability, is an interesting question that remains to be resolved.

[77] Could the calculated variability in the land and ocean CO$_2$ sinks be due to analytical error? The large variability in the early (URI) part of the record would require erroneous drift in the standard curve of about 3 per meg and back again over a period of about 2 years. Smaller errors in the standard curve would be required for the latter (Princeton) part of the record. Such errors would be difficult to detect, and it may be that drift in the standard curves contributes to this variability.

4. Summary and Conclusions

[78] We document methods used for the high-precision mass spectrometric analysis of the O$_2$/N$_2$ ratio of air. The mass spectrometry itself is straightforward; more challenging is achieving protocols for sample handling, standardization, and replicability giving the required precision. Appropriate techniques are described.

[79] We have used our results to partition CO$_2$ uptake to the land biosphere and the ocean between 1993 and 2003. According to our results, ocean uptake was 1.7 ± 0.5 (2.1 ± 0.5) Gt C yr^{-1} between 1994 and 2003 (1993 and 2003), and land uptake was 0.8 ± 0.6 (1.0 ± 0.6) Gt C yr^{-1} during these periods. The first number is based on data from Cape Grim, Barrow, and Samoa, while the value in parentheses is based on Cape Grim only. Ocean uptake agrees with estimates from diverse methods, but is at the lower end. Much of the discrepancy can be resolved by invoking a higher correction, 0.6 Gt C yr^{-1} rather than 0.3, for the effect of ocean O$_2$ outgassing.

[80] Interannual variability in land biosphere and ocean uptake, calculated from O$_2$ data, are compromised by ocean-atmosphere exchange. There seem to be O$_2$ fluxes with periods of a few years superimposed on the secular trend due to outgassing. Nevertheless O$_2$/N$_2$ variations still retain an embedded signal due to variability in sequestration. The close coupling between total sequestration (calculated from the CO$_2$ balance alone) and land biosphere sequestration (from CO$_2$ and O$_2$ constraints) between 1996 and 2001 validate earlier conclusions that high atmospheric CO$_2$ growth rates during most El Niño events are due to a large land source.

References

Andreev, A., and S. Watanabe (2002), Temporal changes in dissolved oxygen of the intermediate water in the subarctic North Pacific, *Geophys. Res. Lett.*, 29(14), 1680, doi:10.1029/2002GL015021.

Battle, M., M. L. Bender, P. P. Tans, J. W. C. White, J. T. Ellis, T. Conway, and R. J. Francey (2000), Global carbon sinks and their variability inferred from atmospheric and d^{13}C, *Science*, 287, 2467–2470.

Bender, M. L., P. P. Tans, J. T. Ellis, J. Orchardo, and K. Habfast (1994), A high-precision isotope ratio mass-spectrometry method for measuring the O$_2$/N$_2$ ratio of air, *Geochim. Cosmochim. Acta*, 58, 4751–4758.

Bender, M., T. Ellis, P. Tans, R. Francey, and D. Lowe (1996), Variability in the/ratio of Southern Hemisphere air, 1991–1994: Implications for the carbon cycle, *Global Biogeochem. Cycles*, 10, 9–21.

Bindoff, N. L., and T. J. McDougall (2000), Decadal changes along an Indian Ocean section at 32° and their interpretation, *J. Phys. Oceanogr.*, 30, 1207–1222.

Bopp, L., C. Le Quere, M. Heimann, A. C. Manning, and P. Monfray (2002), Climate-induced oceanic oxygen fluxes: Implications for the contemporary carbon budget, *Global Biogeochem. Cycles*, 16(2), 1022, doi:10.1029/2001GB001445.

Bousquet, P., P. Peylin, P. Ciais, C. LeQuere, P. Friedlingstein, and P. P. Tans (2000), Regional changes in carbon dioxide fluxes of land and oceans since 1980, *Science*, 290, 1342–1346.

Clark, D. A., S. C. Piper, C. D. Keeling, and D. B. Clark (2003), Tropical rain forest tree growth and atmospheric carbon dynamics linked to interannual temperature variation during 1984–2000, *Proc. Natl. Acad. Sci. U. S. A.*, 100, 5282–5287.

Cleveland, W. S., and S. J. Devlin (1988), Locally weighted regression—An approach to regression-analysis by local fitting, *J. Am. Stat. Assoc.*, 83, 596–610.

Conway, T. J., P. P. Tans, L. S. Waterman, K. W. Thoning, D. R. Kitzis, K. A. Masarie, and N. Zhang (1994), Evidence for interannual variability of the carbon cycle from the NOAA/CMDL global air sampling network, *J. Geophys. Res.*, 99, 22,831–22,855.

Emerson, S., S. Mecking, and J. Abell (2001), The biological pump in the subtropical North Pacific Ocean: Nutrient sources, Redfield ratios, and recent changes, *Global Biogeochem. Cycles*, 15, 535–554.

Feely, R. A., et al. (2002), Seasonal and interannual variability of CO$_2$ in the equatorial Pacific, *Deep Sea Res., Part II*, 49, 2443–2469.

Intergovernmental Panel on Climate Change (2001), *Climate Change 2001, Contribution of Working Group I to the Third Assessment Report of the Intergovernmental Panel on Climate Change*, edited by L. Pitelka and A. Ramirez Rojas, pp. 183–237, Cambridge Univ. Press, New York.

Gurney, K. R., et al. (2003), TransCom3 CO2 inversion intercomparison: 1. Annual mean control results and sensitivity to transport and prior flux information, *Tellus, Ser. B*, 55, 555–579.

Kalnay, E., et al. (1996), The NCEP/NCAR 40-year reanalysis project, *Bull. Am. Meteorol. Soc.*, 77, 437–471.

Keeling, C. D., R. B. Bacastow, A. F. Carter, S. C. Piper, T. P. Whorf, M. Heimann, W. G. Mook, and H. Roeloffzen (1989), A three-dimensional model of atmospheric CO2 transport based on observed winds: 1. Analysis of observational data, in *Aspects of Climate Variability in the Pacific and the Western Americas*, Geophys. Monogr. Ser., vol. 55, edited by D. H. Person, pp. 165–236, AGU, Washington, D. C.

Keeling, R. F. (1988), Development of an interferometric oxygen analyzer for precise measurement of the atmospheric O$_2$ mole fraction, Ph.D. thesis, Harvard University, Cambridge, Mass.

Keeling, R. F., and H. E. Garcia (2002), The change in oceanic O2 inventory associated with recent global warming, *Proc. Natl. Acad. Sci. U. S. A.*, 99, 7848–7853.

Keeling, R. F., and S. R. Shertz (1992), Seasonal and interannual variations in atmospheric oxygen and implications for the global carbon cycle, *Nature*, 358, 723–727.

Keeling, R. F., R. P. Najjar, M. L. Bender, and P. P. Tans (1993), What atmospheric oxygen measurements can tell us about the global carbon cycle, *Global Biogeochem. Cycles*, 7, 37–67.

Keeling, R. F., S. C. Piper, and M. Heimann (1996), Global and hemispheric CO$_2$ sinks deduced from changes in atmospheric O-2 concentration, *Nature*, 391, 218–221.

Keeling, R. F., A. C. Manning, E. M. McEvoy, and S. R. Shertz (1998), Methods for measuring changes in atmospheric O$_2$ concentration and their application in Southern Hemisphere air, *J. Geophys. Res.*, 103, 3381–3397.

Keller, K., R. D. Slater, M. Bender, and R. M. Key (2002), Possible biological or physical explanations for decadal scale trends in North Pacific nutrient concentrations and oxygen utilization, *Deep Sea Res., Part II*, 49, 345–362.

Langenfelds, R. L., R. J. Francey, and L. P. Steele (1999), Partitioning of the global CO$_2$ sink using a 19-year trend in atmospheric O$_2$, *Geophys. Res. Lett.*, 26, 1897–1900.

BENDER ET AL.: ATMOSPHERIC O$_2$/N$_2$ CHANGES, 1993–2002

Langenfelds, R. L., R. J. Francey, B. C. Pak, L. P. Steele, J. Lloyd, C. M. Trudinger, and C. E. Allison (2002), Interannual growth rate variations of atmospheric CO$_2$ and its δ^{13}C, H$_2$, CH$_4$, and CO between 1992 and 1999 linked to biomass burning, *Global Biogeochem. Cycles*, *16*(3), 1048, doi:10.1029/2001GB001466.

Lee, K., R. Wanninkhof, T. Takahashi, S. C. Doney, and R. A. Feely (1998), Low interannual variability in recent oceanic uptake of atmospheric carbon dioxide, *Nature*, *396*, 155–159.

Le Quéré, C., J. C. Orr, P. Monfray, and O. Aumont (2000), Interannual variability of the oceanic sink of CO$_2$ from 1979 through 1997, *Global Biogeochem. Cycles*, *14*, 1247–1265.

Le Quere, C., et al. (2003), Two decades of ocean CO$_2$ sink and variability, *Tellus, Ser. B*, *55*, 649–656.

Levitus, S., J. I. Antonov, T. P. Boyer, and C. Stephens (2000), Warming of the world ocean, *Science*, *287*, 2225–2229.

Ludwig, W., and J.-L. Probst (1996), Predicting the oceanic input of organic carbon by continental erosion, *Global Biogeochem. Cycles*, *10*, 23–41.

Manning, A. C. (2001), Temporal variability of atmospheric oxygen from both continuous measurements and a flask sampling network: Tools for studying the global carbon cycle, Ph. D. thesis, Univ. of Calif., San Diego, La Jolla.

Manning, A. C., R. F. Keeling, and J. P. Severinghaus (1999), Precise atmospheric oxygen measurements with a paramagnetic oxygen analyzer, *Global Biogeochem. Cycles*, *13*, 1107–1115.

Manning, A. C., R. F. Keeling, L. E. Katz, W. J. Paplawsky, and E. M. McEvoy (2003), Interpreting the seasonal cycles of atmospheric oxygen and carbon dioxide concentrations at American Samoa Observatory, *Geophys. Res. Lett.*, *30*(6), 1333, doi:10.1029/2001GL014312.

Marland, G., T. A. Boden, and R. J. Andres (2003), Global, regional, and national fossil fuel co2 emissions, in *Trends: A Compendium of Data on Global Change*, Carbon Dioxide Inf. Anal. Cent., Oak Ridge Natl. Lab., Oak Ridge, Tenn.

Matear, R. J., A. C. Hirst, and B. I. McNeil (2000), Changes in dissolved oxygen in the Southern Ocean with climate change, *Geochem. Geophys. Geosyst.*, *1*, doi:10.1029/2000GC000086.

McKinley, G. A., M. J. Follows, J. Marshall, and S. M. Fan (2003), Interannual variability of air-sea O$_2$ fluxes and the determination of CO$_2$ sinks using atmospheric O$_2$/N$_2$, *Geophys. Res. Lett.*, *30*(3), 1101, doi:10.1029/2002GL016044.

McKinley, G. A., M. J. Follows, and J. Marshall (2004), Mechanisms of air-sea CO$_2$ flux variability in the equatorial Pacific and the North Atlantic, *Global Biogeochem. Cycles*, *18*, GB2011, doi:10.1029/2003GB002179.

McNeil, B. I., R. J. Matear, R. M. Key, J. L. Bullister, and J. L. Sarmiento (2003), Anthropogenic CO$_2$ uptake by the ocean based on the global chlorofluorocarbon data set, *Science*, *299*, 235–239.

Nemani, R. R., C. D. Keeling, H. Hashimoto, W. M. Jolly, S. C. Piper, C. J. Tucker, R. B. Myneni, and S. W. Running (2003), Climate-driven increases in global terrestrial net primary production from 1982 to 1999, *Science*, *300*, 1560–1563.

Pahlow, M., and U. Riebesell (2000), Temporal trends in deep ocean Redfield ratios, *Science*, *287*, 831–833.

Plattner, G. K., F. Joos, and T. F. Stocker (2002), Revision of the global carbon budget due to changing air-sea oxygen fluxes, *Global Biogeochem. Cycles*, *16*(4), 1096, doi:10.1029/2001GB001746.

Rayner, P. J., I. G. Enting, R. J. Francey, and R. Langenfelds (1999), Reconstructing the recent carbon cycle from atmospheric CO$_2$, δ^{13}C and O$_2$/N$_2$ observations, *Tellus, Ser. B*, *51*, 213–232.

Reichenau, T., and G. Esser (2003), Interannual fluctuation of atmospheric CO$_2$ dominated by combined effects of ENSO and volcanic aerosols?, *Global Biogeochem. Cycles*, *17*(4), 1094, doi:10.1029/2002GB002025.

Rodenbeck, C., S. Houweling, M. Gloor, and M. Heimann (2003), Time-dependent atmospheric CO$_2$ inversions based on interannually varying tracer transport, *Tellus, Ser. B*, *55*, 488–497.

Sarmiento, J. L., and E. T. Sundquist (1992), Revised budget for the oceanic uptake of anthropogenic carbon dioxide, *Nature*, *356*, 589–593.

Sarmiento, J. L., T. M. Hughes, R. L. Stouffer, and S. Manabe (1998), Simulated response of the ocean carbon cycle to anthropogenic climate warming, *Science*, *393*, 245–249.

Schaefer, K., A. S. Denning, N. Suits, J. Kaduk, I. Baker, S. Los, and L. Prihodko (2002), Effect of climate on interannual variability of terrestrial CO$_2$ fluxes, *Global Biogeochem. Cycles*, *16*(4), 1102, doi:10.1029/2002GB001928.

Schimel, D. S., et al. (2001), Recent patterns and mechanisms of carbon exchange by terrestrial ecosystems, *Nature*, *414*, 169–172.

Severinghaus, J. P. (1995), Studies of the terrestrial O2 and carbon cycle in sand dune gases and in Biosphere 2, Ph. D. thesis, Columbia Univ., New York.

Shaffer, G. O., O. Leth, O. Ulloa, J. Bendtsen, V. Dellarossa, S. Hormazabal, and P.-I. Sehlstedt (2000), Warming and circulation change in the eastern South Pacific Ocean, *Geophys. Res. Lett.*, *27*, 1247–1250.

Stephens, B. B., R. F. Keeling, M. Heimann, K. D. Six, R. Murnane, and K. Caldeira (1998), Testing global ocean carbon cycle models using measurements of atmospheric O$_2$ and CO$_2$ concentration, *Global Biogeochem. Cycles*, *12*, 213–230.

Stephens, B. B., R. F. Keeling, and W. J. Paplawsky (2003), Shipboard measurements of atmospheric oxygen using a vacuum-ultraviolet absorption technique, *Tellus, Ser. B*, *55*, 857–878.

Sturm, P., M. Leuenberger, C. Sirignano, R. E. M. Neubert, H. A. J. Meijer, R. Langenfelds, W. A. Brand, and Y. Tohjima (2004), Permeation of atmospheric gases through Viton O-rings used for flask sampling, *J. Geophys. Res.*, *109*, D04309, doi:10.1029/2003JD004073.

Takahashi, T., et al. (2002), Global sea-air flux based on climatological surface ocean pCO$_2$, and seasonal biological and temperature effects, *Deep Sea Res., Part II*, *49*, 1601–1622.

Thoning, K. W., P. P. Tans, and W. D. Komhyr (1989), Atmospheric carbon dioxide at Mauna Loa Observatory: 2. Analysis of the NOAA GMCC data, 1974–1985, *J. Geophys. Res.*, *94*, 8549–8565.

Tohjima, Y. (2000), Method for measuring changes in the atmospheric O$_2$/N$_2$ ratio by a gas chromatograph equipped with a thermal conductivity detector, *J. Geophys. Res.*, *105*, 14,575–14,584.

Tohjima, Y., H. Mukai, T. Machida, and Y. Nojiri (2003), Gas-chromatographic measurements of the atmospheric oxygen/nitrogen ratio at Hateruma Island and Cape Ochi-ishi, Japan, *Geophys. Res. Lett.*, *30*(12), 1653, doi:10.1029/2003GL017282.

van der Werf, G. R., J. T. Randerson, G. J. Collatz, L. Giglio, R. S. Kashibhatla, A. F. Arellano Jr., S. C. Olsen, and E. S. Kasischke (2004), Continental-scale partitioning of fire emissions during the 1997 El Niño/La Niña period, *Science*, *303*, 73–76.

————————————

M. O. Battle, Department of Physics and Astronomy, Bowdoin College, 8800 College Station, Brunswick, ME 04011, USA.

M. L. Bender, N. Cassar, D. T. Ho, M. B. Hendricks, R. Mika, and B. Sturtevant, Department of Geoscience, Guyot Hall, Princeton University, Princeton, NJ 08544, USA. (bender@princeton.edu)

T. J. Conway and P. P. Tans, Climate Monitoring and Diagnostics Laboratory, National Oceanic and Atmospheric Administration, Boulder, CO 80305, USA.
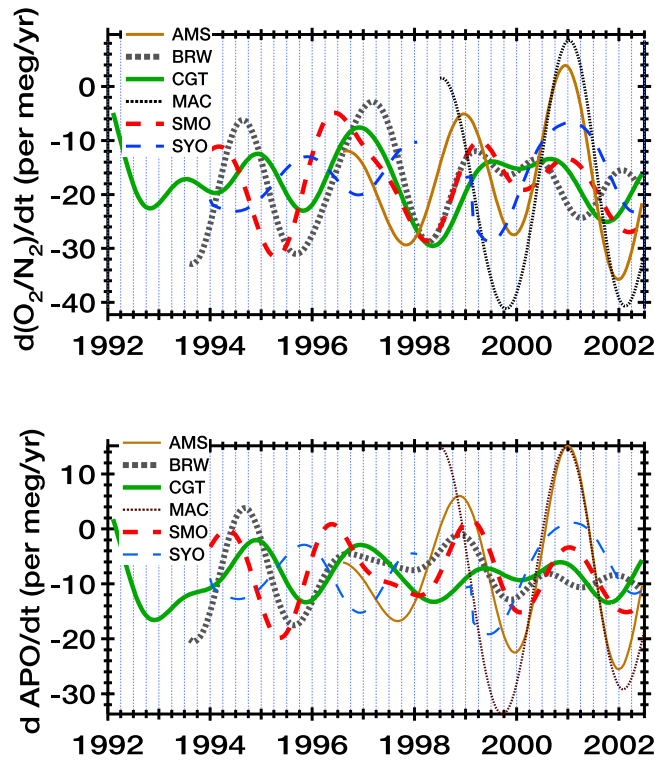
Figure 6. Rates of change of O$_2$/N$_2$ (top) and APO (bottom) in smoothed deseasonalized records from our study sites.
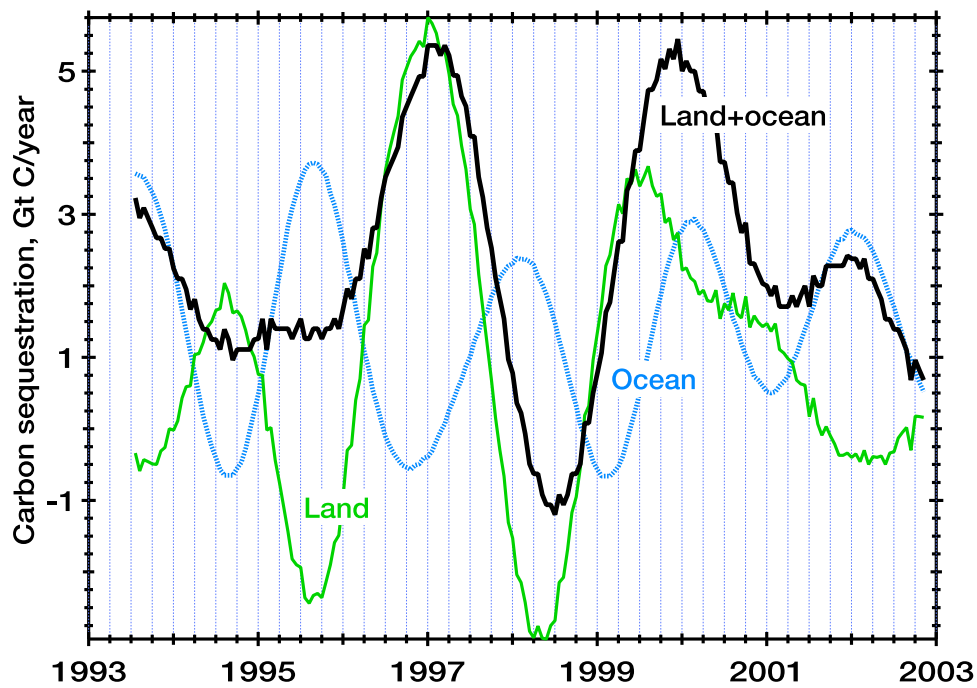

Figure 7. Land and ocean CO$_2$ sequestration rates calculated from CO$_2$ and O$_2$/N$_2$ data at CGO, SMO, and BRW.